Food Chemistry: X 12 (2021) 100169

Contents lists available at ScienceDirect

Food Chemistry: X

journal homepage: www.sciencedirect.com/journal/food-chemistry-x

Purification, chemical analysis and inhibitory effects on galectin-3 of enzymatic pH-modified citrus pectin

Tao Zhang [a,b,1], Guoqing Sun [c,1], Ming Shuai [b], Jingyu Ye [b], Jian Huang [a,b], Xiaodong Yao [c], Chengxin Sun [c,*], Xun Min [a,b,*]

[a] Department of Laboratory Medicine, Affiliated Hospital of Zunyi Medical University, Zunyi 563003, China
[b] School of Laboratory Medicine, Zunyi Medical University, Zunyi 563006, China
[c] School of Pharmacy, Zunyi Medical University, Zunyi 563006, China

ARTICLE INFO

Keywords:
Modified citrus pectin
Polygalacturonase hydrolysis
Purification
Chemical analysis
Galectin-3 inhibitor

ABSTRACT

Modified citrus pectin (MCP), a commercially available dietary supplement prepared from citrus pectin, contains several different polysaccharide domains, but its primary chemical structure and the binding epitopes that antagonize galectin-3 function remain unclear. In this study, five fractions were isolated from MCP after endo-polygalacturonase degradation (EMCP) and a combination of DEAE-cellulose and Sepharose CL-6B or Sephadex G-75 chromatography. Their primary structures, abilities to inhibit galectin-3-mediated hemagglutination, and antiproliferation activities on MCF-7 and A549 cell lines were studied. Results showed that EMCP-3p, one of the five fractions, was composed of Glc (89.8%), Gal (3.8%), Ara (3.1%), GalA (1.1%), Man (0.9%), and Rha (1.3%) with an average molecular weight of 88.4 KDa, which had the most substantial degree of galectin-3 inhibition with an MIC of 31.25 μg/mL, and it exhibited remarkable cytotoxicity against MCF-7 (36.7%) and A549 (57.4%) cell lines. These results provide new insight into the structure–function relationships of EMCP-derived polysaccharides.

Introduction

Pectin, a biomacromolecule present in plant cell walls, is a structural complex polysaccharide rich in galacturonic acid (GalA). Pectin usually contains four structural domains: homogalacturonan (HG), rhamnogalacturonan I (RG-I), rhamnogalacturonan II (RG-II), and xylogalacturonan (XGA) (Maxwell, Belshaw, Waldron, & Morris, 2012). The HG domain, known as the "smooth region" of pectin, is a linear polymer composed of α-(1 → 4)-D-GalA residues, which are usually found to be partially methylesterified at the C-6 position and acetylated at the C-2 or C-3 positions. RG-I, known as the "hairy region" of pectin, consists of a main chain of alternating α-Rha and α-GalA repeat units [-4)-α-GalA-(1 → 2)-α-Rha-(1]$_n$, which is highly branched with α-Ara- and β-Gal-rich side chains linked at C-4 of Rha in the backbone. RG-II, a highly complex branched structure pectin domain, consists of a 9 or 10 α-(1 → 4)-GalA unit main chain and four different branched saccharide β chains linked at C-2 or C-3 of GalA in the backbone (Maxwell et al., 2012; Mohnen, 2008; Perez, 2003; Ridley, O'Neill, & Mohnen, 2001; Willats, Knox, & Mikkelsen, 2006; Yapo, 2011).

The application of pectin in the food industry is usually limited due to its large size and cannot be absorbed by human, so some approaches have been applied to break it down into smaller fragments that can be fermented by gut microbiota. The most studied pH-modified pectin is obtained from citrus, named pH-modified citrus pectin (MCP). One of these pH modification steps is an alkaline treatment, which causes β-elimination reactions, resulting in depolymerization and de-esterification of GalA residues in the pectin backbone. The other step is acid treatment, which cleaves and releases neutral saccharide branches from RG domains in the pectin backbone (Eliaz & Raz, 2019; Glinsky & Raz, 2009).

Cancer is one of the major threats to human health, with an estimated 19.3 million new cancer cases (excluding nonmelanoma skin cancer) and 9.9 million cancer deaths in 2020 (Sung et al., 2021). Galectin-3 (Gal-3), a β-galactoside-binding lectin, has a C-terminal carbohydrate recognition domain (CRD) connected to a long *N*-terminal collagen-like proline- and glycine-rich tail (Argüeso & Panjwani, 2011;

* Corresponding authors at: Department of Laboratory Medicine, Affiliated Hospital of Zunyi Medical University, Zunyi 563003, China (X. Min).
E-mail addresses: 267003388@qq.com (C. Sun), minxun001@hotmail.com (X. Min).
[1] Contributed equally.

https://doi.org/10.1016/j.fochx.2021.100169
Received 6 July 2021; Received in revised form 9 November 2021; Accepted 22 November 2021
Available online 23 November 2021

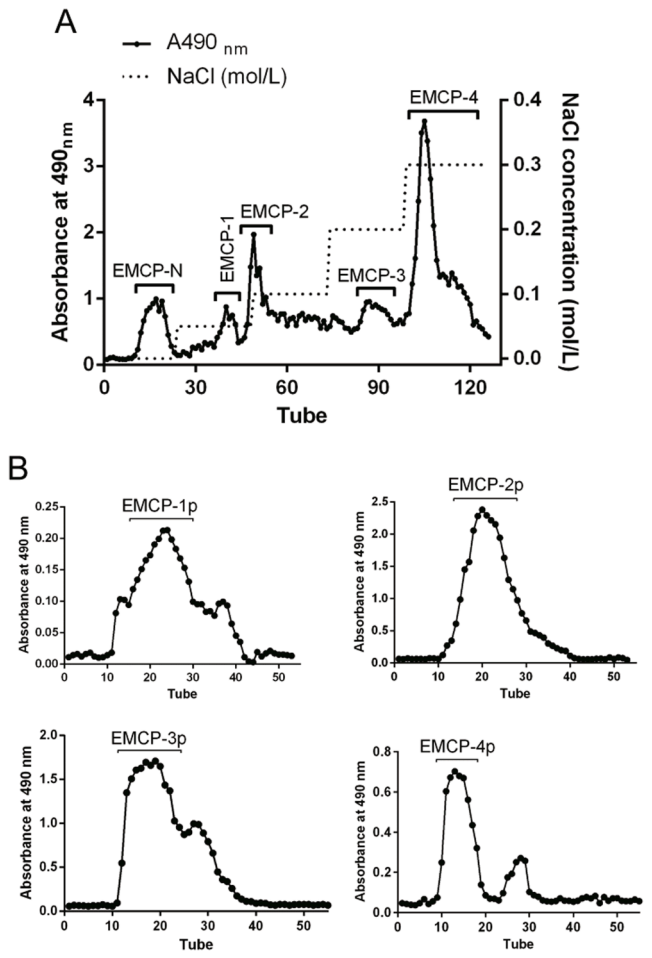

Fig. 1. Elution profile of EMCP on DEAE-cellulose and gel-permeation chromatography. (A) EMCP was applied to a DEAE-cellulose column, and five fractions of EMCP were eluted, initially using dH_2O (EMCP-N), followed by NaCl(aq) at different concentrations of 0.05 M (EMCP-1), 0.1 M (EMCP-2), 0.2 M (EMCP-3), and 0.3 M (EMCP-4). (B) EMCP-1, EMCP-2, and EMCP-3 were applied to a Sephadex G-75 column, and EMCP-4 was applied to a Sepharose CL-6B column.

Barondes et al., 1994; Gao et al., 2012; R. Y. Yang, Rabinovich, & Liu, 2008). The biological functions of Gal-3 are due to the specific binding of glycoconjugates with its carbohydrate recognition domain (Laaf, Bojarova, Elling, & Kren, 2019). Gal-3 is associated with the development and malignancy of cancers, and it has been identified as a "culprit molecule" in different stages of cancer progression, acting to promote the proliferation, adhesion, and metastasis of several types of cancers while also inhibiting cancer cell apoptosis (Blanchard, Yu, Collins, & Bum-Erdene, 2014; Liu & Rabinovich, 2005; Ruvolo, 2015; Song et al., 2014). In addition, tumor cell immune escape is also associated with Gal-3-induced immune cell apoptosis (Hsu, Chen, & Liu, 2009). Thus, Gal-3 has become an important molecular target in the development of anticancer therapeutics.

It has been reported that MCP can bind to the CRD on Gal-3 and exhibit anticancer activity both *in vitro* and *in vivo*, such as metastatic cell cycle arrest in target organs, inhibiting angiogenesis and invasion, and enhancing cancer cell apoptosis in response to cytotoxic drugs (Blanchard et al., 2014; Eliaz & Raz, 2019; Glinsky & Raz, 2009; Zhang, Xu, & Zhang, 2015). However, compared with the large number of biological activity studies of MCP, its structure has been less studied. Yifa Zhou's and Guihua Tai's laboratories tried to fractionate MCP into dozens of homogeneous subfractions and found that RG-I-rich subfractions with β-(1 → 4)-D-galactan side chains were more active than the other RG-I-rich and HG-rich subfractions, e.g., MCP-2a, a homogeneous subfraction, exhibited the greatest inhibitory effect with an MIC (minimum inhibitory concentration) of 12.5 ± 0.6 μg/mL (Zhang et al., 2016). However, all of these homogeneous subfractions contained notable amounts of GalA residues (MCP-2a contained 35.1% GalA), which might affect their binding to Gal-3. In this study, five subfractions were isolated from MCP after *endo*-polygalacturonase hydrolysis, and their primary structures, abilities to inhibit galectin-3-mediated hemagglutination, and antiproliferation activities against MCF-7 and A549 cell lines were studied.

Materials and methods

Materials

Citrus pectin (Reagent grade) was obtained from Kuerhuaxue Company (Beijing, China). Endo-polygalacturonase (≥5 units/mg), various dextrans (1 KDa–2000 KDa, analytical standard for GPC), and eight monosaccharides (glucuronic acid (GlcA, ≥95%), glucose (Glc, ≥98%), galacturonic acid (GalA, ≥98%), galactose (Gal, ≥99%), arabinose (Ara, ≥98%), fucose (Fuc, ≥98%), rhamnose (Rha, ≥98%), and mannose (Man, ≥98%)), were purchased from Sigma. Sepharose CL-6B and Sephadex G-75 were purchased from Amersham Pharmacia Biotech Company. Recombinant human Gal-3 was prepared in our laboratory as previously reported (Zhou et al., 2020). All other reagents were of analytical grade and were purchased in China.

Preparation and purification of enzymatic MCP (EPCP)

MCP was obtained from CP using pH modification as previously described by our laboratory (Zhang et al., 2020). Briefly, the CP solution was treated with NaOH(aq) for 1 h at pH 10.0 followed by HCl(aq) for 12 h at pH 3.0, and the solution was neutralized by NaOH(aq). MCP was precipitated by adding ethanol to the solution up to 70%. MCP (5 g) was dissolved in 200 mL sodium acetate buffer (25 mmol/L, pH 4.2) and incubated with Endo-PG (50 U) at 50 °C for 2 h at static condition. This MCP solution was digested twice again by Endo-PG under the same conditions. The hydrolysates were dialyzed (MWCO 1 kDa) and freeze-dried to yield enzymatic MCP (EMCP) .

EMCP (1 g) dissolved in 100 mL distilled water was applied to a DEAE-cellulose column (2.6 cm × 50 cm), eluted with distilled water to give the neutral fraction (EMCP-N) and then eluted with 0.05 mol/L, 0.1 mol/L, 0.2 mol/L and 0.3 mol/L NaCl(aq) to obtain four acidic fractions (EMCP-1, EMCP-2, EMCP-3, and EMCP-4). The acidic fractions (EMCP-1, EMCP-2, EMCP-3, and EMCP-4) were further purified on a Sepharose CL-6B (1.0 cm × 60 cm) column or a Sephadex G-75 (1.0 cm × 60 cm) column, which was eluted with 0.15 mol/L NaCl, and the flow rate was 0.1 mL/min. The total sugar content of each tube (1.2 mL) was detected by phenol–sulfuric acid assay, and the appropriate eluates were collected, dialyzed, and freeze-dried to obtain four fractions (EMCP-1p, EMCP-2p, EMCP-3p, and EMCP-4p).

Monosaccharide composition analysis

The polysaccharide sample (2 mg) was degraded first with 2 mol/L CH_3OH-HCl for 16 h at 80 °C followed by 2 mol/L TFA(aq) for 1 h at 120 °C. The degradation products were derivatized by using 1-phenyl-3-methyl-5-pyrazolone (PMP), and the derivatives were detected using an HPLC system (LC-10AD, Shimadzu) containing an SPD-10AV detector, two LC-10AD pumps and a DIKMA Inertsil ODS-3 column (4.6 mm × 150 mm, 5 μm). The column was eluted with 18.0% acetonitrile and 82.0% PBS buffer (0.1 mol/L, pH 7.0) (V/V) at a flow rate of 1.0 mL/min and detected at 245 nm (Zhang et al., 2020).

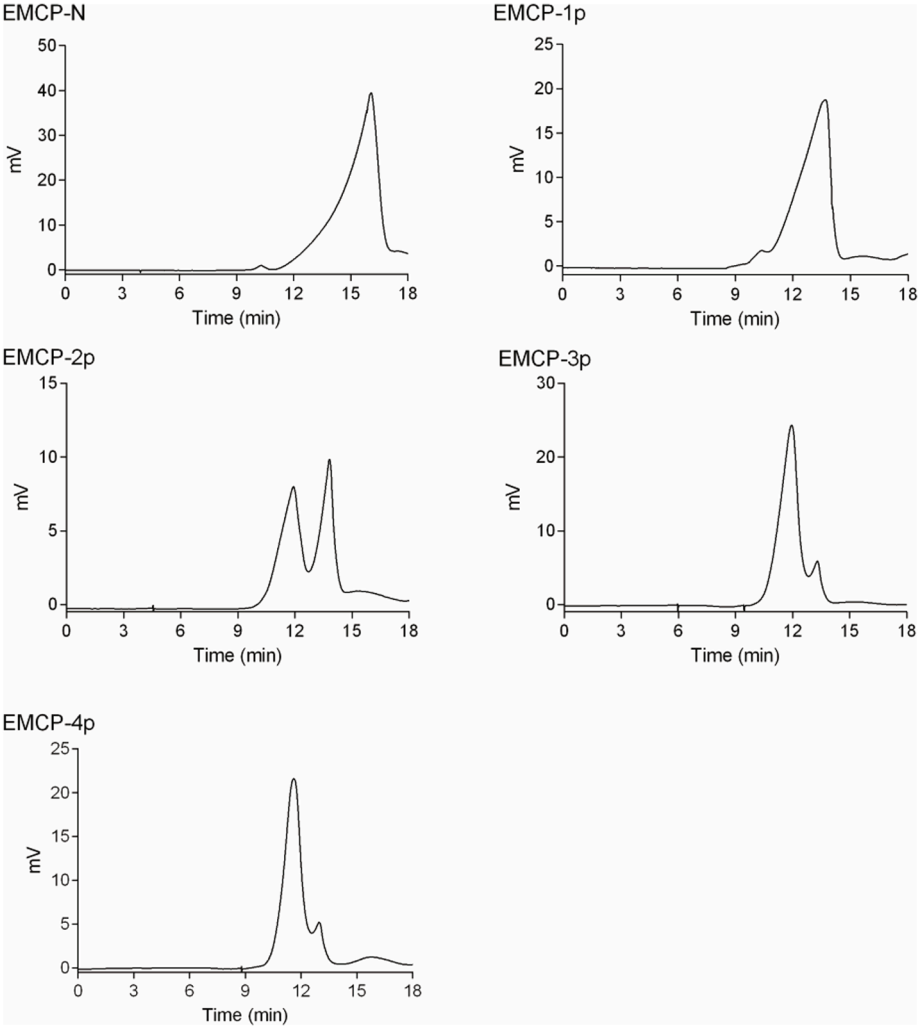

Fig. 2. Homogeneity and average molecular weight of the EMCP fractions.

Homogeneity and molecular weight analysis

The molecular weights were analyzed by gel-permeation chromatography on a Waters Ultrahydrogel 250 column (7.8 × 300 mm, Waters Corporation, Milford, Massachusetts, USA) coupled to a Shimadzu HPLC system and a Schambeck RI2000A refractive index detector as described previously (Zhang et al., 2020). The columns were precalibrated by standard dextrans (1 KDa, 5 KDa, 10 KDa, 50 KDa, 2000 KDa), and the molecular weights of the EMCP fractions were calculated by linear regression analysis.

Thiobarbituric acid method

The thiobarbituric acid (TBA) method was performed according to a previously published protocol (Karkhanis, Zeltner, Jackson, & Carlo, 1978). In brief, each polysaccharide sample was treated with 0.1 mol/L H_2SO_4 at 100 °C for 0.5 h to release 3-deoxy-D-mannooct-2-ulosonic acid (Kdo). The hydrolysates were reacted with $NaAsO_2$, periodic acid, and thiobarbituric acid, and dimethylsulfoxide was added to the solution at 25 °C. If the polysaccharide sample contained Kdo, a red chromophore would be produced and could be detected.

FT-IR analysis

The polysaccharide sample was mixed with dried KBr powder, and this mixture was pressed into a 1-mm pellet. An FT-IR instrument (Bruker Tensor 27) was used to obtain the spectra ranging from 400 cm^{-1} to 4000 cm^{-1}. The resolution was 4 cm^{-1}, and scan number was 32.

NMR analysis

A polysaccharide sample (20 – 30 mg) was dissolved in 1 mL D_2O (99.8%), and a Bruker AV600 spectrometer (Karlsruhe, Germany) was used to give the ^{13}C NMR spectrum at 25 °C. Acetone was used as an internal standard.

Gal-3-mediated hemagglutination method

The Gal-3-mediated hemagglutination method was carried out as previously described (Zhou et al., 2020). In brief, a transparent microplate (V type) was used in this experiment, and each well of this microplate contained 25 μL 0.15 mol/L NaCl (control) or 25 μL polysaccharide sample solution, 25 μL 1% bovine serum albumin (BSA) dissolved in 0.15 mol/L NaCl, 25 μL 15 μg/mL Gal-3 solution (PBS, pH 7.4), and 25 μL 4% (V/V) chicken erythrocyte suspension (PBS, pH 7.4). After standing for 0.5 h at 25 °C, the concentrations of the polysaccharide samples that could completely inhibit the aggregation of the chicken erythrocytes were recorded, and the minimum inhibitory concentration (MIC) was used to describe its binding affinity to Gal-3.

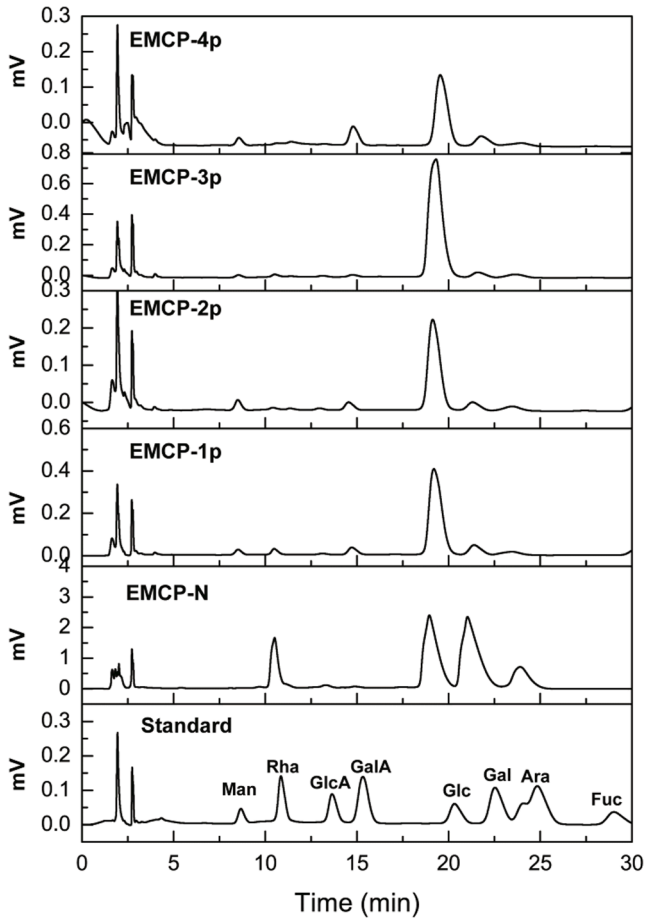

Fig. 3. Monosaccharide compositions of the EMCP fractions.

Anti-proliferation activity assay

Both MCF-7 cell lines (human breast cancer, DMEM with 10% FBS) and A549 cell lines (human lung carcinoma, RPMI 1640 with 10% FBS) were used to determine the antiproliferative activity of the EMCP fractions. The MCF-7 and A549 cell lines were both incubated at 37 °C and 5% CO_2. In brief, each well of a 96-well plate was seeded with MCF-7 or A549 cells (5×10^3 per well in 100 μL media) and incubated for 24 h, and then 100 μL of each EMCP fraction at serial concentrations (4000 μg/mL, 2000 μg/mL, 1000 μg/mL, 500 μg/mL, 250 μg/mL, 125 μg/mL) was added to each well. After 48 h of incubation, 20 μL of MTT (5 mg/mL) was added to each well, followed by incubation for another 4 h. After removing the culture medium, 150 μL DMSO was added to each well, and a microplate reader (Thermo, USA) was used to detect the absorbance at 490 nm. The antiproliferative effect of the EMCP fractions was calculated as follows:

Cell viabilities (% control)=$(A_2\text{-}A_0)/(A_1\text{-}A_0) \times 100$, where A_0 is the absorbance of the system containing culture medium; A_1 is the absorbance of the system with cells; A_2 is the absorbance of the system with the EMCP fraction.

Statistical analysis

All data obtained from the *in vitro* experiment are expressed as the mean ± SEM. One-way ANOVA was used to analyze the data, and Dunnett's test was then compared with the control group (SPSS 19 software, IBM Corporation, USA). A *P*-value less than 0.05 was defined as statistical significance.

Results and discussion

EMCP preparation and purification

MCP was obtained from CP using pH modification as previously described by our laboratory (Zhang et al., 2020), and EMCP (yield 42.0%) was obtained from MCP using Endo-PG hydrolysis. As shown in Fig. 1A, EMCP (1 g) dissolved in 100 mL dH_2O was added to a DEAE–cellulose column (2.5 cm × 50 cm), which was eluted with dH_2O to obtain one neutral fraction (EMCP-N, yield 2.9%), followed by elution with 0.05 mol/L, 0.1 mol/L, 0.2 mol/L and 0.3 mol/L NaCl to obtain four acidic fractions (EMCP-1, EMCP-2, EMCP-3, and EMCP-4). As shown in Fig. 1B, the acidic fractions (EMCP-1, EMCP-2, EMCP-3, and EMCP-4) were further purified on a Sepharose CL-6B (1.0 cm × 60 cm) column or a Sephadex G-75 (1.0 cm × 60 cm) column, which was eluted with 0.15 mol/L NaCl at 0.1 mL/min. Based on the elution profile, the appropriate eluates were collected, dialyzed, and freeze-dried to obtain four purified fractions: EMCP-1p (0.8%), EMCP-2p (2.3%), EMCP-3p (1.8%), and EMCP-4p (19.6%). In addition to the purification of MCP by chromatography, do Prado et al. (2019) fractionated MCP by sequential ultrafiltration using 30, 10, and 3 kDa MWCO Amicon Ultra-4 Centrifugal Filters based on different molecular weights to give four fractions: MCP30 (68%), MCP 30/10 (15%), MCP10/3 (10%), and MCP3 (7%).

Homogeneity and average molecular weight of the EMCP fractions

The homogeneity and average molecular weight of each fraction were determined by HPGPC on a Waters Ultrahydrogel 250 column. As shown in Fig. 2, EMCP-N, EMCP-1p, EMCP-3p, and EMCP-4p each yielded a major single peak, suggesting that they were homogeneous, and their average molecular weights were estimated to be 3.1 KDa, 21.2 KDa, 88.4 KDa, and 117 kDa, respectively. EMCP-2p gave multiple peaks, indicating that it was heterogeneous, and we did not purify it further. The average molecular weight was estimated to be 19.3 KDa-90.8 KDa. Compared to the sequential ultrafiltration method, the average molecular weight of MCP30/10 (10–30 kDa), MCP30 (>30 kDa), and MCP10/3 (3–10 kDa) obtained by do Prado et al. (2019) were smaller than that of EMCP fractions.

Monosaccharide compositions of the EMCP fractions

The monosaccharide compositions of these fractions are provided in Fig. 3. EMCP-N was composed of Glc (39.9%), Gal (34.4%), Ara (12.5%), and Rha (13.2%); EMCP-1p was composed of Glc (77.4%), Gal (8.7%), Ara (4.3%), GalA (4.5%), Man (2.5%), and Rha (2.6%); EMCP-2p was composed of Glc (78.4%), Gal (7.2%), Ara (4.8%), GalA (4.9%), and Man (4.7%); EMCP-3p was composed of Glc (89.8%), Gal (3.8%), Ara (3.1%), GalA (1.1%), Man (0.9%), and Rha (1.3%); and EMCP-4p was composed of Glc (67.0%), Gal (10.2%), Ara (4.9%), GalA (13.8%), and Man (4.1%). The acidic fractions mainly consisted of neutral monosaccharide residues (such as Glc, Gal, Ara, Man), while their content of GalA was much lower, which showed that the HG domains of MCP were removed by Endo-PG hydrolysis. Compared to the sequential ultrafiltration method, the amount of GalA of MCP30/10, MCP30, and MCP10/3 obtained by do Prado et al. (2019) was much higher than that of EMCP fractions, which might be due to the limited hydrolysis using *endo*-polygalacturonase. Wu et al (2020) used *endo*-polygalacturonase hydrolysis to remove nearly half of the GalA residues from 49.8% in EP-1 to 26.47% in EP-2. Besides, after enzymatic hydrolysis, EP-2 showed much higher amount of Glc residues as compared to WSP.

FT-IR spectra of the EMCP fractions

FT-IR spectroscopy, one of the principal methods used to study the basic structure of complex polysaccharides, was utilized to analyze the

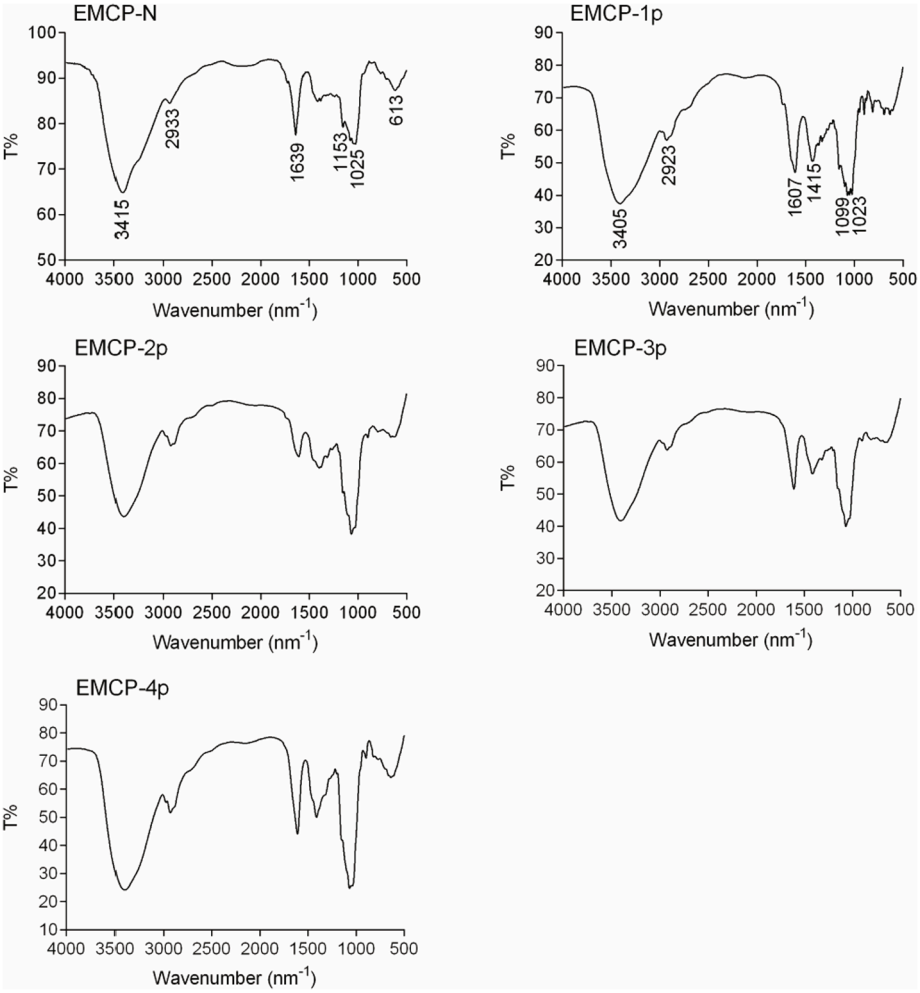

Fig. 4. FT-IR spectra of the EMCP fractions.

EMCP fractions. As shown in Fig. 4, the FT-IR spectra of the EMCP fractions were indistinguishable, with only slight differences in their intensity of absorption. The strong absorption at approximately 3415 cm^{-1} and 3405 cm^{-1} by the EMCP fractions suggests that these fractions contained hydroxy groups, and the absorption at approximately 2933 cm^{-1} and 2923 cm^{-1} were attributed to methyl or methylene groups, which are both structural features of polysaccharides. In addition, the absorption at approximately 1607 cm^{-1} was attributed to the C═O bonds in the acidic polysaccharide fractions, and the absorption at approximately 1639 cm^{-1} was attributed to the C—O group in EMCP-N (Ji et al., 2019; Liang et al., 2019); the absorption at approximately 1415 cm^{-1} was attributed to the C—H group; and the absorption at 1023 cm^{-1} and 1099 cm^{-1} suggested that EMCP-1, EMCP-2, EMCP-3, and EMCP-4 all contained some uronic acid. The absorption at approximately 1025 cm^{-1} indicated that EMCP-N contains some arabinogalactan–related domains (Capek et al., 2003), and absorption at 1153 cm^{-1} was related to C—O stretching vibration of 6-OH owing to Glc or/and Gal residues (Coimbra, Barros, Barros, Rutledge, & Delgadillo, 1998; Zhang et al., 2020); the absorption at approximately 613 cm^{-1} was due to the pyranose rings of polysaccharides (Zhang et al., 2019).

Inhibitory activities of EMCP fractions on Gal-3-mediated hemagglutination

The Gal-3-mediated hemagglutination method is usually performed to analyze the inhibitory activities of Gal-3 inhibitors. The MIC value is utilized to quantify the activity of the inhibitor toward complete inhibition of hemagglutination. This assay was carried out as described previously (Zhou et al., 2020). The inhibitory activities of the EMCP fractions are shown in Fig. 5A. EMCP-N, EMCP-1p, EMCP-2p, EMCP-3p and EMCP-4p exhibited different activities; in particular, EMCP-3p exhibited the strongest inhibition with a MIC of 31.25 μg/mL, followed by EMCP-2p with a MIC of 125 μg/mL. EMCP-N, EMCP-1p and EMCP-4p exhibited the weakest inhibition with the same MIC of 250 μg/mL. Compared to MCP-2a reported by Zhang et al., the MIC value of EMCP-3p was slightly higher than that of MCP-2a (MIC 12.5 μg/mL) (Zhang et al., 2016), which suggested that the HG domain could be important in MCP activity by maintaining the structural conformation of the entire molecule (Gao et al., 2013).

Anti-proliferation activities

Gal-3 can promote the proliferation and migration of some cancer cells, so the MTT method was utilized to analyze the inhibitory activities of EMCP fractions on Gal-3. The antiproliferative effects of the EMCP fractions were evaluated on MCF-7 and A549 cell lines *in vitro*. As shown in Fig. 5B, the viabilities of the MCF-7 and A549 cells were clearly inhibited by all EMCP fractions in a concentration-dependent manner. The five fractions exhibited cell viability in this order: EMCP-3p (36.7%) > EMCP-4p (45.9%) > EMCP-N (53.4%) > EMCP-2p (55.4%) > EMCP-1p (56.9%) against MCF-7 cells and EMCP-2p (53.4%) > EMCP-3p (57.4%) > EMCP-1p (64.8%) > EMCP-4p (82.8%) > EMCP-N (89.3%) against A549 cells. Especially at a concentration of 2.0 mg/mL EMCP-3p, the viability of MCF-7 cells (36.7%) was much lower than

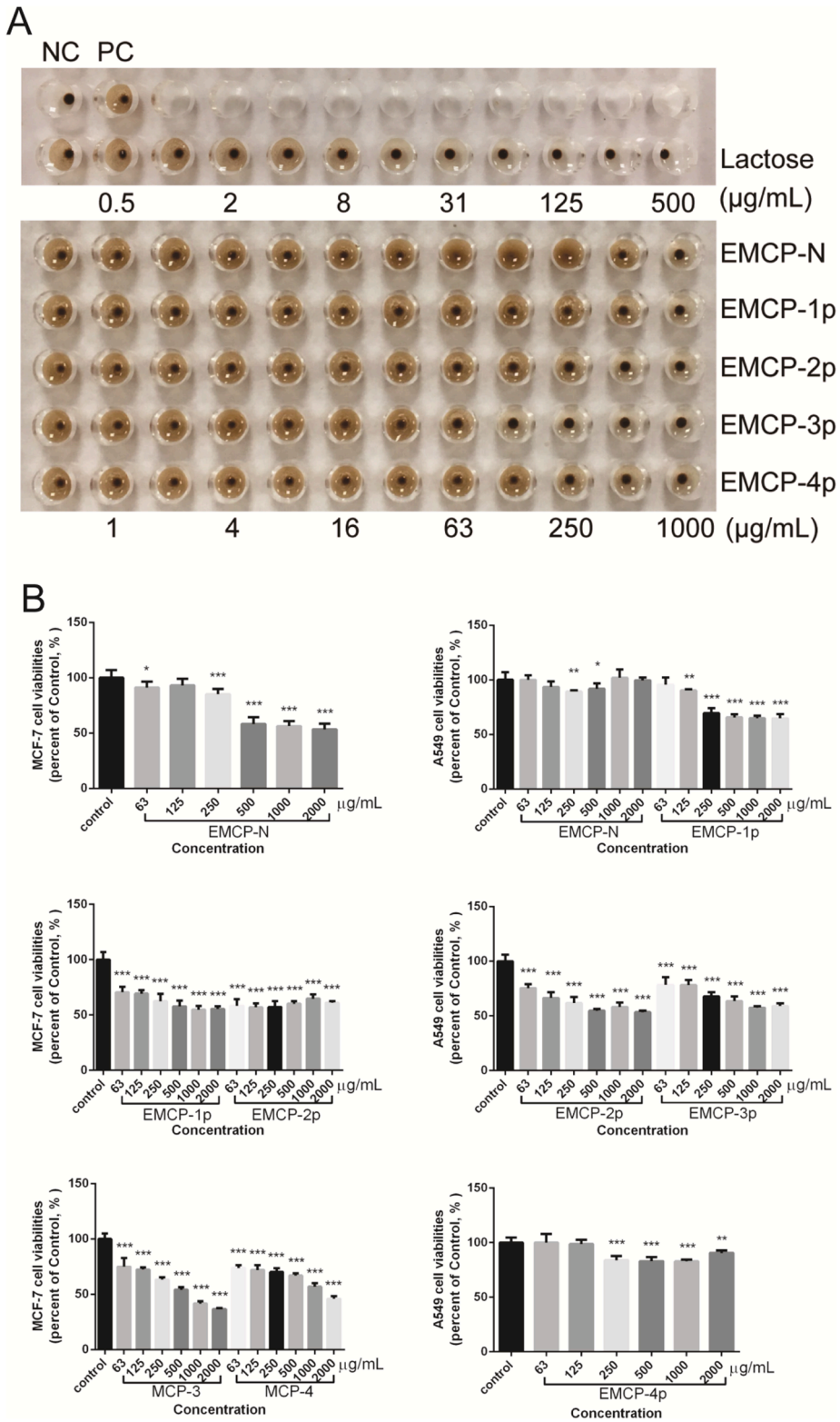

Fig. 5. Assessment of the inhibitory effects of EMCP fractions on Gal-3 function. (A) Hemagglutination assays. NC, negative control; PC, positive control. (B) Effects on MCF-7 (A) and A549 (B) cell line viability. Means with different letters are significantly different (*P* less than 0.05), and error bars represent SEM.

that of A549 cells (57.4%), suggesting that A549 cells are less sensitive to Gal-3 inhibitors, which may be due to the lower expression level of Gal-3 in A549 cell lines than in MCF-7 cells (Wei et al., 2019; Wu et al., 2020).

These results suggest that the EMCP fractions could exert antitumor activity as Gal-3 antagonists against some cancer cells with high expression levels of Gal-3, indicating the potential of EMCP fractions for curing some cancers, especially EMCP-3p. Compared to pectin or polysaccharides prepared from other plants, the anti-proliferation effect of EMCP-3p against MCF-7 cell lines was stronger than that of *Dictyophora indusiata* polysaccharide (Liao et al., 2015), *Angelica sinensis* polysaccharide (Zhang et al., 2016), and pectin from citrus canning

processing water (WSP) (Wu et al., 2020). The antiproliferative effect of EMCP-2p against A549 cells was stronger than that of *Flammulina velutipes* polysaccharide (Yang et al., 2012) and WSP (Wu et al., 2020). The results obtained above suggested the potential antitumor activities of EMCP-3p and EMCP-2p.

Among the EMCP fractions, EMCP-3p and EMCP-2p showed remarkable Gal-3 inhibition effects and antiproliferation effects, so we used ^{13}C NMR experiments to analyze their primary structures. As shown in Supplementary Fig. 1., the NMR spectra of EMCP-2p and EMCP-3p were complex, and most of the resonances from C-2 to C-5 might not be assigned accurately, while the C-1 resonances of some saccharide residues could be assigned. For example, the resonance at 106.79 ppm could be assigned to C-1 of Ara, and the resonances ranging from 103.52 ppm to 104.14 ppm could be assigned to C-1 of Gal and/or Man residues. The resonances at 99.06 ppm and 170.94 ppm were attributed to C-1 and C-6 of GalA residues, respectively (Catoire, Goldberg, Pierron, Morvan, & Du Penhoat, 1998). Resonances of C-1 from Glc residues could be identified, and resonances at 102.28 ppm and 100.47 ppm represented β-(1 → 6)-Glc and β-(1 → 4,6)-Glc residues, respectively (Zhang et al., 2016). The signals at 95.65 ppm and 34.06 ppm could be attributed to C-2 and C-3 of Kdo residues, respectively (Wu et al., 2018; Zhang et al., 2016). Kdo residues present in EMCP-2p were also verified by a positive result with the TBA assay. Kdo, linked to the HG chain, indicated that some Kdo residues through the C-3 of GalA are linked to the HG chain (Perez, 2003). Kdo residues were not detected in EMCP-2p, which could be due to nonreducing monosaccharides (such as Kdo) not reacting with PMP to avoid detection (Honda, Suzuki, & Taga, 2003).

Kdo residues present in the HG chain are reminiscent of the RG-II domain. The RG-II domain is composed of an HG main chain and four side chains, and two of the side chains are linked to the HG main chain via Api residues, while the other two side chains are linked to HG through Kdo or Dha (Perez, 2003). EMCP-2p contains Kdo, Api, AceA and GalA residues, which suggests that it may contain some RG-II domains. Zhang et al. reported that MCP-3Sb, one fraction purified from pH-modified citrus pectin, only contained Kdo and GalA residues, which showed little inhibitory effect on the Gal-3-mediated hemagglutination assay as compared to MCP-3P, containing only GalA residues, suggesting that Kdo residues could attenuate the inhibitory effect of polysaccharide on Gal-3 functions (Zhang et al., 2016). In this study, we also observed that the MIC value of EMCP-2p was much higher than that of EMCP-3p. In addition, the antiproliferative effects of EMCP-2p against A549 cell lines were slightly stronger than those of EMCP-3p, which could be because the expression level of Gal-3 in MCF-7 cell lines is higher than that in A549 cell lines.

Conclusion

In conclusion, five polysaccharide components (EMCP-N, EMCP-1p, EMCP-2p, EMCP-3p, and EMCP-4p) were prepared from MCP after *endo*-polygalacturonase degradation followed by fractionation using DEAE-cellulose and Sephadex G-75 or Sepharose CL-6B chromatography. Among these fractions, EMCP-3p was mainly composed of Glc (89.8%), Gal (3.8%), Ara (3.1%), etc.; with an average molecular weight of 88.4 KDa, it exhibited the strongest Gal-3 inhibition with a MIC of 31.25 μg/mL and exhibited remarkable antiproliferation effects against MCF-7 (36.7%) and A549 (57.4%) cell lines compared to most other pectins and polysaccharides. Thus, we suggest that these results provide new insight into the structure–activity relationships of EMCP-derived polysaccharides and provide a reference for developing EMCP-based Gal-3 inhibitors with low toxicity.

Declaration of Competing Interest

The authors declare that they have no known competing financial interests or personal relationships that could have appeared to influence the work reported in this paper.

Acknowledgments

This work was supported by the National Natural Science Foundation of China (No. 32060035), the Technology Research and Development Program of Guizhou (No. qiankehezhicheng [2018]2803), the Program for Excellent Young Talents of Zunyi Medical University (No. 18zy-006).

Appendix A. Supplementary data

Supplementary data to this article can be found online at https://doi.org/10.1016/j.fochx.2021.100169.

References

Argüeso, P., & Panjwani, N. (2011). Focus on Molecules: Galectin-3. *Experimental Eye Research, 92*(1), 2–3.
Barondes, S. H., Castronovo, V., Cooper, D., Cummings, R. D., Drickamer, K., Feizi, T., & Kasai, K. (1994). Galectins: A family of animal beta-galactoside-binding lectins. *Cell, 76*(4), 597–598.
Blanchard, H., Yu, X., Collins, P. M., & Bum-Erdene, K. (2014). Galectin-3 inhibitors: A patent review (2008–present). *Expert Opinion on Therapeutic Patents, 24*(10), 1053–1065.
L. Catoire R. Goldberg M. Pierron C. Morvan C. Herv du Penhoat An efficient procedure for studying pectin structure which combines limited depolymerization and 13C NMR European Biophysics Journal 27 2 1998 127 136.
Capek, P., Hříbalová, V., Švandová, E., Ebringerová, A., Sasinková, V., & Masarová, J. (2003). Characterization of immunomodulatory polysaccharides from *Salvia officinalis* L. *International Journal of Biological Macromolecules, 33*(1-3), 113–119.
Coimbra, M. A., Barros, A., Barros, M., Rutledge, D. N., & Delgadillo, I. (1998). Multivariate analysis of uronic acid and neutral sugars in whole pectic samples by FT-IR spectroscopy. *Carbohydrate Polymers, 37*(3), 241–248.
do Prado, S. B. R., Shiga, T. M., Harazono, Y., Hogan, V. A., Raz, A., Carpita, N. C., & Fabi, J. P. (2019). Migration and proliferation of cancer cells in culture are differentially affected by molecular size of modified citrus pectin. *Carbohydrate Polymers, 211*, 141–151.
Eliaz, I., & Raz, A. (2019). Pleiotropic Effects of Modified Citrus Pectin. *Nutrients, 11*(11), 2619.
Gao, X., Liu, D., Fan, Y., Li, X., Xue, H., Ma, Y., … Hong, W. (2012). The Two Endocytic Pathways Mediated by the Carbohydrate Recognition Domain and Regulated by the Collagen-like Domain of Galectin-3 in Vascular Endothelial Cells. *PloS One, 7*(12), e52430.
Gao, X., Zhi, Y., Sun, L., Peng, X., Zhang, T., Xue, H., … Zhou, Y. (2013). The Inhibitory Effects of a Rhamnogalacturonan I (RG-I) Domain from Ginseng Pectin on Galectin-3 and Its Structure-Activity Relationship. *Journal of Biological Chemistry, 288*(47), 33953–33965.
Glinsky, V. V., & Raz, A. (2009). Modified citrus pectin anti-metastatic properties: One bullet, multiple targets. *Carbohydrate Research, 344*(14), 1788–1791.
Honda, S., Suzuki, S., & Taga, A. (2003). Analysis of carbohydrates as 1-phenyl-3-methyl-5-pyrazolone derivatives by capillary/microchip electrophoresis and capillary electrochromatography. *Journal of Pharmaceutical and Biomedical Analysis, 30*(6), 1689–1714.
Hsu, D. K., Chen, H. Y., & Liu, F. T. (2009). Galectin-3 regulates T-cell functions. *Immunological Reviews, 230*(1), 114–127.
Ji, X., Zhang, F., Zhang, R., Liu, F., Peng, Q., & Wang, M. (2019). An acidic polysaccharide from Ziziphus Jujuba cv. Muzao: Purification and structural characterization. *Food Chemistry, 274*, 494–499.
Karkhanis, Y. D., Zeltner, J. Y., Jackson, J. J., & Carlo, D. J. (1978). A new and improved microassay to determine 2-keto-3-deoxyoctonate in lipopolysaccharide of Gram-negative bacteria. *Analytical Biochemistry, 85*(2), 595–601.
Laaf, D., Bojarová, P., Elling, L., & Křen, V. (2019). Galectin-Carbohydrate Interactions in Biomedicine and Biotechnology. *Trends in Biotechnology, 37*(4), 402–415.
Liang, X.-X., Gao, Y.-Y., Pan, Y., Zou, Y.-F., He, M., He, C.-L., … Lv, C. (2019). Purification, chemical characterization and antioxidant activities of polysaccharides isolated from Mycena dendrobii. *Carbohydrate Polymers, 203*, 45–51.
Liao, W., Lu, Y., Fu, J., Ning, Z., Yang, J., & Ren, J. (2015). Preparation and Characterization of Dictyophora indusiata Polysaccharide-Zinc Complex and Its Augmented Antiproliferative Activity on Human Cancer Cells. *Journal of Agricultural and Food Chemistry, 63*(29), 6525–6534.
Liu, F.-T., & Rabinovich, G. A. (2005). Galectins as modulators of tumour progression. *Nature Reviews Cancer, 5*(1), 29–41.
Maxwell, E. G., Belshaw, N. J., Waldron, K. W., & Morris, V. J. (2012). Pectin – An emerging new bioactive food polysaccharide. *Trends in Food Science & Technology, 24*(2), 64–73.
MOHNEN, D. (2008). Pectin structure and biosynthesis. *Current Opinion in Plant Biology, 11*(3), 266–277.
Perez, S. (2003). A complex plant cell wall polysaccharide: Rhamnogalacturonan II. A structure in quest of a function. *Biochimie, 85*(1–2), 109–121.
Ridley, B. L., O'Neill, M. A., & Mohnen, D. (2001). Pectins: Structure, biosynthesis, and oligogalacturonide-related signaling. *Phytochemistry, 57*(6), 929–967.

Ruvolo, P. P. (2015). Galectin 3 as a guardian of the tumor microenvironment. *Biochimica et Biophysica Acta (BBA) - Molecular. Cell Research, 1863*(3), 427–437.
Song, L., Tang, J.-w., Owusu, L., Sun, M.-Z., Wu, J., & Zhang, J. (2014). Galectin-3 in cancer. *Clinica Chimica Acta, 431*, 185–191.
Sung, H., Ferlay, J., Siegel, R. L., Laversanne, M., Soerjomataram, I., Jemal, A., & Bray, F. (2021). *Global cancer statistics 2020: GLOBOCAN estimates of incidence and mortality worldwide for 36 cancers in 185 countries*. CA: A Cancer Journal for Clinicians.
Wei, C., Zhang, Y.u., He, L., Cheng, J., Li, J., Tao, W., … Chen, S. (2019). Structural characterization and anti-proliferative activities of partially degraded polysaccharides from peach gum. *Carbohydrate Polymers, 203*, 193–202.
Willats, W. G. T., Knox, J. P., & Mikkelsen, J. D. (2006). Pectin: New insights into an old polymer are starting to gel. *Trends in Food Science & Technology, 17*(3), 97–104.
Wu, D.i., Cui, L., Yang, G., Ning, X., Sun, L., & Zhou, Y. (2018). Preparing rhamnogalacturonan II domains from seven plant pectins using Penicillium oxalicum degradation and their structural comparison. *Carbohydrate Polymers, 180*, 209–215.
Wu, D., Zheng, J., Hu, W., Zheng, X., He, Q., Linhardt, R. J., … Chen, S. (2020). Structure-activity relationship of Citrus segment membrane RG-I pectin against Galectin-3: The galactan is not the only important factor. *Carbohydrate Polymers, 245*, 116526. https://doi.org/10.1016/j.carbpol.2020.116526
Yang, R. Y., Rabinovich, G. A., & Liu, F. T. (2008). Galectins: Structure, function and therapeutic potential. *Expert Reviews in Molecular Medicine, 10*, Article e17.
Yang, W., Pei, F., Shi, Y., Zhao, L., Fang, Y., & Hu, Q. (2012). Purification, characterization and anti-proliferation activity of polysaccharides from Flammulina velutipes. *Carbohydrate Polymers, 88*(2), 474–480.
Yapo, B. M. (2011). Rhamnogalacturonan-I: A Structurally Puzzling and Functionally Versatile Polysaccharide from Plant Cell Walls and Mucilages. *Polymer Reviews, 51*(4), 391–413.
Zhang, T., Lan, Y.u., Zheng, Y.i., Liu, F., Zhao, D., Mayo, K. H., … Tai, G. (2016). Identification of the bioactive components from pH-modified citrus pectin and their inhibitory effects on galectin-3 function. *Food Hydrocolloids, 58*, 113–119.
Zhang, T., Shuai, M., Ma, P., Huang, J., Sun, C., Yao, X., … Yan, S. (2020). Purification, chemical analysis and antioxidative activity of polysaccharides from pH-modified citrus pectin after dialyzation. *LWT - Food Science and Technology, 128*, 109513. https://doi.org/10.1016/j.lwt.2020.109513
Zhang, W., Xu, P., & Zhang, H. (2015). Pectin in cancer therapy: A review. *Trends in Food Science & Technology, 44*(2), 258–271.
Zhang, Y.u., Zhou, T., Wang, H., Cui, Z., Cheng, F., & Wang, K.-P. (2016). Structural characterization and in vitro antitumor activity of an acidic polysaccharide from Angelica sinensis (Oliv.) Diels. *Carbohydrate Polymers, 147*, 401–408.
Zhang, Z., Lv, G., Cheng, J., Cai, W., Fan, L., & Miao, L. (2019). Characterization and biological activities of polysaccharides from artificially cultivated Phellinus baumii. *International Journal of Biological Macromolecules, 129*, 861–868.
Zhou, L., Ma, P., Shuai, M., Huang, J., Sun, C., Yao, X., … Zhang, T. (2020). Analysis of the water-soluble polysaccharides from Camellia japonica pollen and their inhibitory effects on galectin-3 function. *International Journal of Biological Macromolecules, 159*, 455–460.